

A Class of Regular Biorthogonal Linear-Phase Filterbanks: Theory, Structure, and Application in Image Coding

Soontorn Oraintara, *Member, IEEE*, Trac D. Tran, *Member, IEEE*, and Truong Q. Nguyen, *Senior Member, IEEE*

Abstract—This paper discusses a method of regularity imposition onto biorthogonal linear-phase M -band filterbanks using the lattice structure. A lifting structure is proposed for lattice matrix parameterization where regularity constraints can be imposed. The paper focuses on cases with analysis and synthesis filterbanks having up to two degrees of regularity. Necessary and sufficient conditions for regular filterbanks in terms of the filter impulse response, frequency response, scaling function, and wavelets are revisited and are derived in terms of the lattice matrices. This also leads to a constraint on the minimum filter length. Presented design examples are optimized for the purpose of image coding, i.e., the main objectives are coding gain and frequency selectivity. Simulation results from an image coding application also show that these transforms yield improvement in the perceptual quality in the reconstruction images. The approach has also been extended to the case of integer/rational lifting coefficients, which are desirable in many practical applications.

Index Terms—Biorthogonal filterbanks, GenLOT, integer transforms, lattice structure, regularity, vanishing moment.

I. INTRODUCTION

WAVELETS and filterbanks have established themselves as powerful tools in transform-based signal compression applications [1]. They are used to remove spatial signal redundancy in many video, image, and audio coding standards such as MPEG video, JPEG, and MPEG audio [2]. Fig. 1 shows the general block diagram of a transform-based signal coding algorithm. The input signal is represented as a linear combination of the transform basis functions, and their corresponding coefficients (the so-called transform coefficients) are obtained at the output of the transform block. These coefficients are then efficiently quantized and entropy coded to the coder output. In this paper, we focus on still image coding as an application of transform-based signal compression, whereas other applications can also be naturally applied.

There has been considerable interest in designing the transform that yields high perceptual reconstructed quality while

keeping the computational cost low. At the earlier stage, the discrete cosine transform (DCT) was first employed as an efficient transform for the JPEG image coding standard, where the bases are truncated cosine functions, having equal length, linear phase, orthogonality, and uniform localization in the frequency domain. However, at low bit rates, the reconstruction usually suffers from blocking artifacts due to the discontinuity at the borders of the basis functions. The discrete wavelet transform is a more recent technique employed in transform-based image coder in order to reduce or eliminate blocking artifacts. Constructed by iterating on the lowpass branch of a two-channel perfect reconstruction (PR) filterbank, the entire frequency domain is octavely divided, rendering a multiscale image representation. Perhaps the most popular wavelet filter pair used in practical image coders is the (9/7)-tap linear phase biorthogonal wavelet, which has also been used in the FBI's fingerprint compression standard [3] and now in JPEG2000 [4]. Combining the advantages of efficient implementation of the DCT and the overlapping basis functions of wavelets, lapped transforms (LTs) have been recently studied and found to often outperform the previous two conventional techniques [5]–[7].

The transforms for image coding can be categorized into two major classes: block-based and wavelet-based. Block transforms can be constructed by uniform M -channel filterbanks such as DCT [8], LOT [5], and GenLOT [6], and wavelet transforms can be generated by iterating two-channel filterbanks on the lowpass channel [1]. In transforms of both families, all filter impulse responses have real values with linear-phase (LP) responses (symmetric or anti-symmetric). The linearity of the phase responses is to eliminate the phase distortion and to allow symmetric extension at the border of the image.

Fig. 2(a) shows a uniform maximally decimated M -channel filterbank that consists of the analysis filters $H_i(z)$ and synthesis filters $F_i(z)$. The M -fold downsampling at the analysis side indicates that the total sampling rate at the input of the processing block is equal to that of the original input signal. Fig. 2(b) illustrates the equivalent polyphase structure where $\mathbf{E}(z)$ and $\mathbf{R}(z)$ are the type-I and -II polyphase matrices of the analysis filters $H_i(z)$ and synthesis filters $F_i(z)$, respectively [9]. It is obvious that the filterbank is PR if $\mathbf{E}(z)$ and $\mathbf{R}(z)$ are inverse of each other.

A fundamental concept in wavelet theory is regularity. It should be made clear that the term *regularity* has been used to define the degree of smoothness of the basis functions and the

Manuscript received December 26, 2001; revised March 21, 2003. The associate editor coordinating the review of this paper and approving it for publication was Dr. Helmut Bölcskei.

S. Oraintara is with the University of Texas at Arlington, Department of Electrical Engineering, Arlington, TX 76019-0016 USA (e-mail: oraintar@uta.edu).

T. D. Tran is with the Department of Electrical and Computer Engineering, Johns Hopkins University, Baltimore, MD 21218 USA (e-mail: trac@jhu.edu).

T. Q. Nguyen is with the Department of Electrical and Computer Engineering, University of California San Diego, La Jolla, CA 92093 USA (e-mail: nguyent@ece.ucsd.edu).

Digital Object Identifier 10.1109/TSP.2003.818909

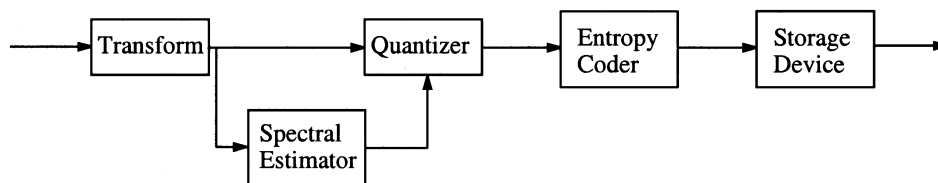
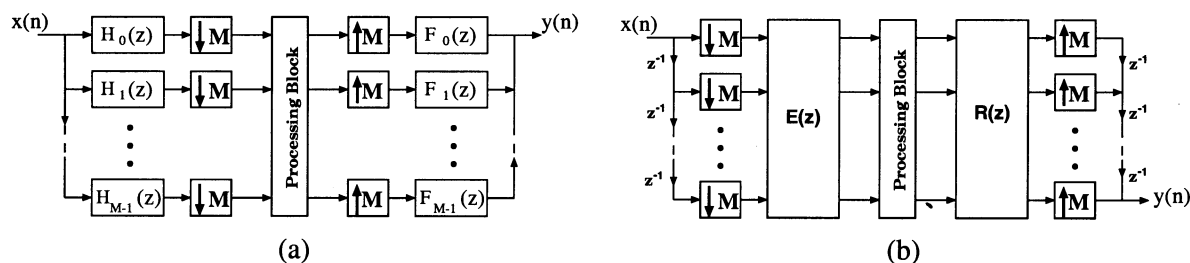


Fig. 1. Block diagram of image coder.

Fig. 2. M -channel filterbank. (a) Regular and (b) Polyphase structures.

number of zeros at aliasing frequencies of the lowpass filter, as pointed out in [1]. They are different but closely related to each other. Indeed, it has been shown that the later is always greater [1]. It is also equivalent to the vanishing moments (number of zeros at dc frequency) of the bandpass filters [10]–[12]. Moreover, when the analysis and synthesis lowpass filters have different numbers of zeros at aliasing frequencies, that of the analysis (synthesis) one will be equal to the vanishing moment of the synthesis (analysis) bank. For the rest of the paper, the term regularity of a transform will be referred to as the number of multiple zeros at the aliasing frequencies and will be used interchangeably with the vanishing moment.

Definition 1: An M -band filterbank is said to be (K_a, K_s) -regular if the analysis and synthesis lowpass filters $H_0(z)$ and $F_0(z)$ have, respectively, at least K_a and K_s zeros at $(2\pi k)/M$ for $k = 1, \dots, M - 1$.

In the paraunitary (PU) case, the degrees of regularity of the analysis and synthesis filterbanks are equal since their impulse responses are time-reversed, and hence, the regularity degree of the filterbank can be identified by using one number instead of an order pair. To be consistent with [13], we will use K -regular for the case of (K, K) -regular PU filterbanks. In the biorthogonal (BO) case, the analysis and synthesis lowpass filters can be different, and thus, their degrees of regularity may not be the same. In particular, for a K -regular PU filterbank, the bandpass filters of the analysis and synthesis filters have K vanishing moments, i.e., $\sum_n n^\ell h_i(n) = 0$ for $\ell = 0, 1, \dots, K - 1$ and $i = 1, 2, \dots, M - 1$. For a (K_a, K_s) -regular BO filterbank, the analysis and synthesis bandpass filters, respectively, have K_s and K_a vanishing moments. (See Proposition 1.)

In image coding application, the analysis filters should be optimized to obtain maximum coding gain, i.e., the magnitude response must match the signal spectrum with high stopband attenuation for maximum decorrelation [14]. On the other hand, the synthesis filters should be optimized to yield smooth basis functions. This can be accomplished by imposing a number of zeros at mirror frequencies into the synthesis lowpass filter. Therefore, the cost functions for the optimization of $H_i(z)$ and

$F_i(z)$ should be different. In the PU case, since $f_i(n)$ are simply the time-reversed versions of $h_i(n)$, they cannot be optimized for different purposes. In the BO case, the frequency responses of $H_0(z)$ and $F_0(z)$ can be different, and they can have different numbers of zeros at mirror frequencies. In practice, $F_0(z)$ should have more zeros in order to obtain smooth synthesis basis functions. At the same time, the analysis bandpass and highpass filters should have a high number of vanishing moments in order to obtain superior energy compaction at a low frequency band. This paper presents a method to impose one and two degrees of regularity into $H_0(z)$ and $F_0(z)$ using lattice structures of BOLP filterbanks.

There are two major conventional approaches in imposing regularity into a filterbank. The first method is to first design the lowpass filters with desired degrees of regularity and then try to optimize the others [11], [15]. It is well known that when $M = 2$, once the lowpass filters are obtained, the other (high-pass) filters can be uniquely identified. However, if $M > 2$, the solutions are not obvious. In [11] and [16], a Gram–Schmidt process is employed in order to orthogonally construct the other filters. This approach, however, does not guarantee linear phase of the filter impulse responses, which is important to many applications. In addition, it is difficult to jointly optimize all the filters simultaneously. The second approach is to impose constraints on the filters' impulse responses [17]. Though straightforward, this approach does not guarantee perfect reconstruction of the resulting filterbank and cause the optimization routine to converge very slowly, and the optimization process can easily get trapped in local minima. Moreover, regularity can only be approximately imposed.

A. Organization

In this paper, we introduce a novel approach of imposing up to two vanishing moments directly onto the lattice structure of M -channel BOLP filterbanks. Section II reviews the lattice structure of BOLP filterbanks. Their relations to the transform's regularity are presented in Section III. In Section IV, a method

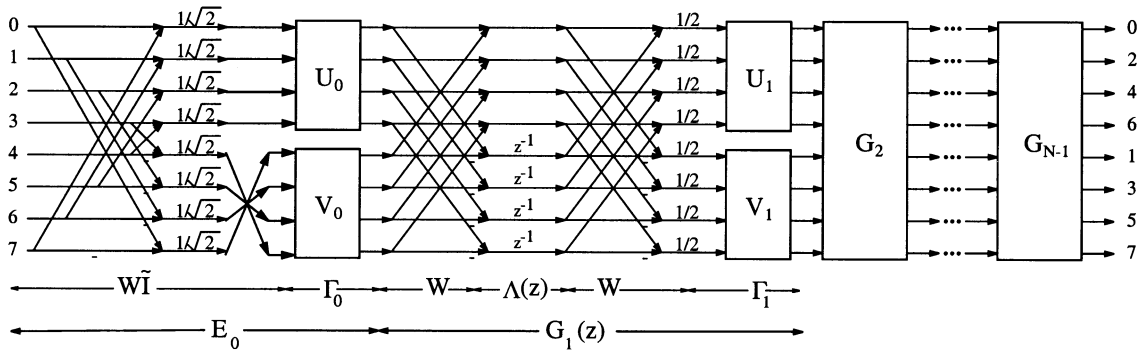


Fig. 3. Lattice structure for linear-phase lapped transform.

for imposing these conditions onto the lattice components is discussed with numerous design examples. Image coding examples are presented in Section V, and Section VI concludes the paper.

B. Notations

Bold-faced lower-case characters are used to denote vectors, whereas bold-faced upper-case characters are used to denote matrices. \mathbf{A}^T , \mathbf{A}^{-1} , and $|\mathbf{A}|$ denote, respectively, the transpose, the inverse, and the determinant of the matrix \mathbf{A} . The symbols $h_i[n]$, $H_i(z)$, and $H_i(e^{j\omega})$ stand for the i th filter's impulse response, its associated z -transform, and its Fourier transform.

Several special matrices with reserved symbols are the polyphase matrix of the analysis bank $\mathbf{E}(z)$, the polyphase matrix of the synthesis bank $\mathbf{R}(z)$, the identity matrix \mathbf{I} , the reversal matrix \mathbf{J} , the null matrix $\mathbf{0}$, a permutation matrix \mathbf{P} , and the diagonal matrix \mathbf{D} with entries being either $+1$ or -1 . Likewise, the special vectors are the column vector with all entries being unity $\mathbf{1}$ and the column vector with all entries being zero, except the first entry being unity \mathbf{a} . When the size of a matrix or vector is not clear from context, subscripts will be included. M and K are usually reserved for the number of channels and the degrees of regularity. An M -channel MN -tap FB is sometimes denoted as an $M \times MN$ lapped transform, where N is the overlapping factor. For abbreviations, we often use LP, PR, PU, and FB to denote *linear phase*, *perfect reconstruction*, *paraunitary*, and *filterbank*.

II. LATTICE STRUCTURE FOR BOLP FILTERBANKS

The lattice structure is an efficient implementation of filterbanks or lapped transforms with linear-phase basis functions [6], [7]. In this paper, it is assumed that the number of channels $M \geq 4$ is even, and all the filters have equal length NM , where N is an integer. It has been proven that when the number of channels is even, there are $M/2$ symmetric and $M/2$ anti-symmetric filters [18]. The polyphase matrix $\mathbf{E}(z)$ is an $M \times M$ polynomial matrix in z of order $(N - 1)$. Under the assumptions on M , N and the filter symmetry, the lattice elements can be defined as follows:

$$\mathbf{\Gamma}_i = \begin{bmatrix} \mathbf{U}_i & \mathbf{0}_L \\ \mathbf{0}_L & \mathbf{V}_i \end{bmatrix}, \quad \mathbf{W} = \frac{1}{\sqrt{2}} \begin{bmatrix} \mathbf{I}_L & \mathbf{I}_L \\ \mathbf{I}_L & -\mathbf{I}_L \end{bmatrix}$$

$$\mathbf{\Lambda}(z) = \begin{bmatrix} \mathbf{I}_L & \mathbf{0}_L \\ \mathbf{0}_L & z^{-1}\mathbf{I}_L \end{bmatrix}, \quad \text{and} \quad \tilde{\mathbf{I}} = \begin{bmatrix} \mathbf{I}_L & \mathbf{0}_L \\ \mathbf{0}_L & \mathbf{J}_L \end{bmatrix}$$

where $L = M/2$, and \mathbf{J} is the reversal matrix. \mathbf{U}_i and \mathbf{V}_i are nonsingular matrices of size $L \times L$. For PU filterbanks, these matrices are orthonormal, and each of them can be parameterized using $\binom{L}{2}$ rotation angles [9]. For BO filterbanks, these \mathbf{U}_i and \mathbf{V}_i matrices are nonsingular, and there are L^2 free parameters in each matrix. The polyphase matrix $\mathbf{E}(z)$ of an LP filterbank with degree $N - 1$ can be factored as a product of nonsingular polynomial matrices with degree one [6], [7], i.e.,

$$\mathbf{E}(z) = \mathbf{G}_{N-1}(z)\mathbf{G}_{N-2}(z)\dots\mathbf{G}_1(z)\mathbf{E}_0 \quad (1)$$

where $\mathbf{G}_i(z) = \mathbf{\Gamma}_i\mathbf{W}\mathbf{\Lambda}(z)\mathbf{W}$, and $\mathbf{E}_0 = \mathbf{\Gamma}_0\mathbf{I}\mathbf{J}\mathbf{W}$. Hence, a causal synthesis polyphase matrix $\mathbf{R}(z)$ can be given by

$$\mathbf{R}(z) = z^{1-N}\mathbf{E}_0^{-1}\mathbf{G}_1^{-1}(z)\dots\mathbf{G}_{N-2}^{-1}(z)\mathbf{G}_{N-1}^{-1}(z). \quad (2)$$

Fig. 3 shows the lattice structure of BOLP filterbanks. Although this structure is minimal in terms of the number of delays, it does not minimize the number of free parameters. In [12] and [19], the authors show that the matrices \mathbf{U}_i for $i > 0$ can be set to \mathbf{I} without any completeness violation. This more-efficient structure with $\mathbf{U}_i \equiv \mathbf{I}$ for $i > 0$ will be used throughout the analysis of this paper.

III. RELATIONSHIP BETWEEN THE LATTICE STRUCTURE AND FILTERBANK'S REGULARITY

The theory of regular M -band wavelets and filterbanks has been well established. Here, we only summarize their important properties. Let us denote $\phi(t)$ and $\psi_i(t)$ ($i = 1, 2, \dots, M - 1$) as the synthesis scaling function and wavelets, and let $\tilde{\phi}(t)$ and $\tilde{\psi}_i(t)$ ($i = 1, 2, \dots, M - 1$) be the analysis scaling function and wavelets. These functions satisfy the dilation and wavelet equations [1] as follows:

$$\tilde{\phi}(t) = M \sum_k h_0(k)\tilde{\phi}(Mt - k) \quad \text{and}$$

$$\phi(t) = M \sum_k f_0(k)\phi(Mt - k)$$

$$\tilde{\psi}_i(t) = M \sum_k h_i(k)\tilde{\phi}(Mt - k) \quad \text{and}$$

$$\psi_i(t) = M \sum_k f_i(k)\phi(Mt - k).$$

Since the filterbank is PR, it is straightforward to show that

$$\begin{aligned} \int \phi(t-k)\tilde{\phi}(t-\ell) dt &= \delta(k-\ell) \\ \int \psi_i(t-k)\tilde{\psi}_j(t-\ell) dt &= \delta(i-j)\delta(k-\ell) \\ \int \phi(t-k)\tilde{\psi}_i(t-\ell) dt &= 0 \\ \int \tilde{\phi}(t-k)\psi_j(t-\ell) dt &= 0. \end{aligned}$$

From Definition 1, the regularity of filterbanks was defined the analysis and synthesis lowpass filters in the frequency domain. The conditions can also be expressed in other forms, as summarized below.

Proposition 1: For a (K_a, K_s) -regular filterbank, the following statements are true.

- 1) The analysis (synthesis) bandpass and highpass filter $H_i(z)$ ($F_i(z)$), $i = 1, 2, \dots, M-1$ have K_s (K_a) multiple zeros at the dc frequency ($z = 1$).
- 2) Polynomial sequences up to degree $K_s - 1$ ($K_a - 1$) are rejected by the analysis (synthesis) bandpass and highpass filters and are captured by the analysis (synthesis) lowpass filter. In other words, we have the following.
 - a) $\sum_n n^k h_i(n) = 0, i = 1, 2, \dots, M-1$, for $0 \leq k \leq K_s - 1$.
 - b) $\sum_n n^k f_i(n) = 0, i = 1, 2, \dots, M-1$, for $0 \leq k \leq K_a - 1$.
- 3) The first K_s (K_a) moments of $\psi_i(t)$ ($\tilde{\psi}_i(t)$) are zero for all $i = 1, 2, \dots, M-1$.
- 4) If $g(t)$ has K_s derivatives, then

$$\left| \int g(t)\tilde{\psi}_i(M^j t - k) dt \right| = O(M^{-jK_s})$$

where O suggests order of its argument [20].

- 5) $\|g(t) - \sum_k a_{jk}\phi(M^j t - k)\| = O(M^{-jK_s})$.
- 6) The downsampling matrix

$$\mathbf{L} = (\downarrow M)\mathbf{M}\mathbf{H}_0 = M \begin{bmatrix} h_0(0) & \dots & h_0(M) & \dots \\ 0 & \dots & h_0(0) & \dots \\ \vdots & \vdots & \vdots & \vdots \end{bmatrix}$$

has eigenvalues $1, 1/M, \dots, (1/M)^{K_a-1}$.

Conditions 1 and 2 express the regularity of the filterbank in terms of the vanishing moments of the bandpass filters in frequency domain and time domain, respectively. These conditions have been translated to the wavelet domain in condition 3. Conditions 4 and 5 relate the regularity to smoothness of these basis functions. The wavelet coefficients decay exponentially proportional to M^{-jK_s} for a sufficiently smooth function $g(t)$, which therefore will be well approximated by the synthesis scaling function with high degree of regularity. Finally, they are expressed in the eigenvalue domain in condition 6. These condi-

tions are useful and can be used to test the regularity of a filterbank in different situations. The proofs of Proposition 1 can be found in the Appendix.

Next, in order to impose the regularity into the lattice structure, equivalent relations in terms of the polyphase matrices need to be established.

Theorem 1: A filterbank is (K_a, K_s) -regular if and only if its polyphase matrices $\mathbf{E}(z)$ and $\mathbf{R}(z)$ satisfy the following conditions:

$$\begin{aligned} \frac{d^n}{dz^n} \{[1 \ z^{-1} \ \dots \ z^{1-M}]\mathbf{E}^T(z^M)\} \Big|_{z=1} \\ = [c_n \ 0 \ \dots \ 0] \end{aligned} \quad (3)$$

$$\begin{aligned} \frac{d^m}{dz^m} \{[1 \ z^{-1} \ \dots \ z^{1-M}]\mathbf{R}(z^M)\} \Big|_{z=1} \\ = [d_m \ 0 \ \dots \ 0] \end{aligned} \quad (4)$$

where $n = 0, \dots, K_s - 1; m = 0, \dots, K_a - 1$, and $\{c_n, d_m\}$ are some nonzero constants [12], [21].

Equations (3) and (4) can be expressed in terms of the lattice elements \mathbf{U}_0 and \mathbf{V}_i . Since the calculation is straightforward but the expressions are very cumbersome, we will present the results only for the cases of (K_a, K_s) -regular BOLP filterbanks with $K_a, K_s \leq 2$. Substituting (1) and (2) into (3) and (4) for the cases of $n, m \leq 1$ yields the following conditions:

$$\begin{aligned} A_{01}(n=0): \mathbf{U}_0 \mathbf{1}_L &= c_0 \mathbf{a}_L \\ A_{10}(m=0): \mathbf{U}_0^{-T} \mathbf{1}_L &= d_0 \mathbf{a}_L \\ A_{02}(n=1): \sqrt{L} \mathbf{a}_L + \sqrt{L} \sum_{j=2}^{N-1} \prod_{i=N-2}^{N-j} \mathbf{V}_i \mathbf{a}_L \\ &+ \prod_{i=N-2}^0 \mathbf{V}_i \mathbf{b}_L = \mathbf{0}_L \\ A_{20}(m=1): \sqrt{L} \mathbf{a}_L + \sqrt{L} \sum_{j=2}^{N-1} \prod_{i=N-2}^{N-j} \mathbf{V}_i^{-T} \mathbf{a}_L \\ &+ \prod_{i=N-2}^0 \mathbf{V}_i^{-T} \mathbf{b}_L = \mathbf{0}_L \end{aligned}$$

where $\mathbf{b}_L = (1/(2L)) [1 \ 3 \ \dots \ 2L-1]^T$. The proof of these conditions can be done directly by substituting the factorization of the polyphase matrices into (3) and (4). Similar derivation for orthogonal case can be found in [13, Appendix], and thus, the proof will be omitted here.

In a (K_a, K_s) -regular filterbank, a combination of the above conditions must be satisfied as shown in the following:

Filterbank	Necessary and sufficient conditions
(1, 1)-regular	A_{01}, A_{10}
(1, 2)-regular	A_{01}, A_{10}, A_{02}
(2, 1)-regular	A_{01}, A_{10}, A_{20}
(2, 2)-regular	$A_{01}, A_{10}, A_{02}, A_{20}$

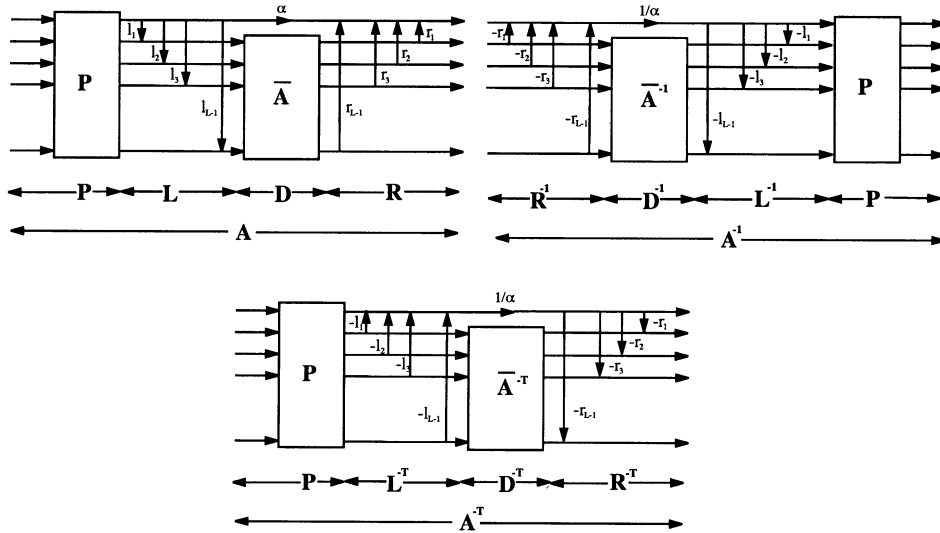


Fig. 4. Lifting parameterization of a nonsingular matrix \mathbf{A} and its inverse.

IV. LATTICE PARAMETERIZATION

In this section, a lifting structure is used to parameterize nonsingular matrices \mathbf{U}_0 and \mathbf{V}_i . This structure has several advantages over the direct and the SVD structures as discussed later in this section.

Lemma 1: Any nonsingular $L \times L$ matrix \mathbf{A} can be decomposed as $\mathbf{A} = \mathbf{RDLP}$, where

$$\mathbf{R} = \begin{bmatrix} 1 & r_1 & r_2 & \cdots & r_{L-1} \\ 0 & 1 & 0 & & 0 \\ 0 & 0 & 1 & & 0 \\ & & & \ddots & \\ 0 & 0 & 0 & \cdots & 1 \end{bmatrix}$$

$$\mathbf{L} = \begin{bmatrix} 1 & 0 & 0 & \cdots & 0 \\ l_1 & 1 & 0 & & 0 \\ l_2 & 0 & 1 & & 0 \\ & & & \ddots & \\ l_{L-1} & 0 & 0 & \cdots & 1 \end{bmatrix}$$

are upper and lower triangular matrices with, respectively, only the first row and column being nonzero, and $\mathbf{D} = \begin{bmatrix} \alpha & \\ & \bar{\mathbf{A}} \end{bmatrix}$ is nonsingular, i.e., $\bar{\mathbf{A}}$ is nonsingular, and $\alpha \neq 0$. Fig. 4 illustrates the parameterization of this matrix \mathbf{A} . The matrix \mathbf{P} is a permutation matrix that switches between the first row and a certain i th row i .

Counting the number of free parameters of \mathbf{A} , we can see that \mathbf{R} and \mathbf{L} have up to $2(L-1)$ nonzero lifting coefficients. The matrix \mathbf{D} has one nonzero multiplication and a $(L-1) \times (L-1)$ matrix $\bar{\mathbf{A}}$, which can be parameterized by another $(L-1)^2$ parameters. Hence, the total number of the free parameters of \mathbf{A} is $1 + 2(L-1) + (L-1)^2 = L^2$, which is equal to that obtained from the direct parameterization or the SVD factorization. Thus, this factorization is minimal in the sense that the number of free parameters is minimized.

The proposed lifting structure provides many advantages over the direct and SVD structures. First, let us compare this with the

direct structure. The new lifting structure offers a robust implementation of the matrix \mathbf{A} with integer coefficients, i.e., the coefficients r_i and l_i can be quantized in both \mathbf{A} and \mathbf{A}^{-1} , and the quantized versions still preserve invertibility between them. The entire matrix \mathbf{A} and its inverse can also be obtained with all integer coefficients if the same structure is repeated in $\bar{\mathbf{A}}$, and so on. On the other hand, in the direct structure, if the elements of \mathbf{A} and \mathbf{A}^{-1} are quantized directly, invertibility is no longer guaranteed.

Now, let us explore the above with the SVD structure, which is a product of two orthogonal matrices and a diagonal matrix in between. Each orthogonal matrix can be implemented using $\binom{L}{2}$ rotation angles. Each angle can be implemented using a butterfly with four floating-point multiplications ($\sin \theta$ and $\cos \theta$). The integer implementation is also possible by converting each butterfly into three lifting steps, and these lifting coefficients can be quantized with invertibility preserved. Each lifting is equivalent to one multiplication, and therefore, for an $L \times L$ matrix, there are $2 \times \binom{L}{2} \times 3 + L = 3L^2 - 2L$ multiplications. On the other hand, in the new lifting structure, each lifting is equivalent to one multiplication, and thus, the number of multiplications is only L^2 . Hence, this new structure is also more efficient from a computational complexity standpoint.

In the remaining of this section, a new method for imposing regularities into a BOLP filterbank is discussed, where each invertible matrix is parameterized using the above lifting structure. In particular, we will demonstrate that one and two vanishing moments can be imposed directly onto the parameters l_i, r_i , and α of the free-parameter matrices \mathbf{U}_0 and \mathbf{V}_i .

A. (1, 1)-Regular Systems

For BOLP systems, the degree of regularity or the number of vanishing moments of the analysis and synthesis lowpass filters are not equal in general, and thus, imposing a number of zeros at dc of the bandpass and highpass analysis filters does not imply that the synthesis bandpass and highpass filters will

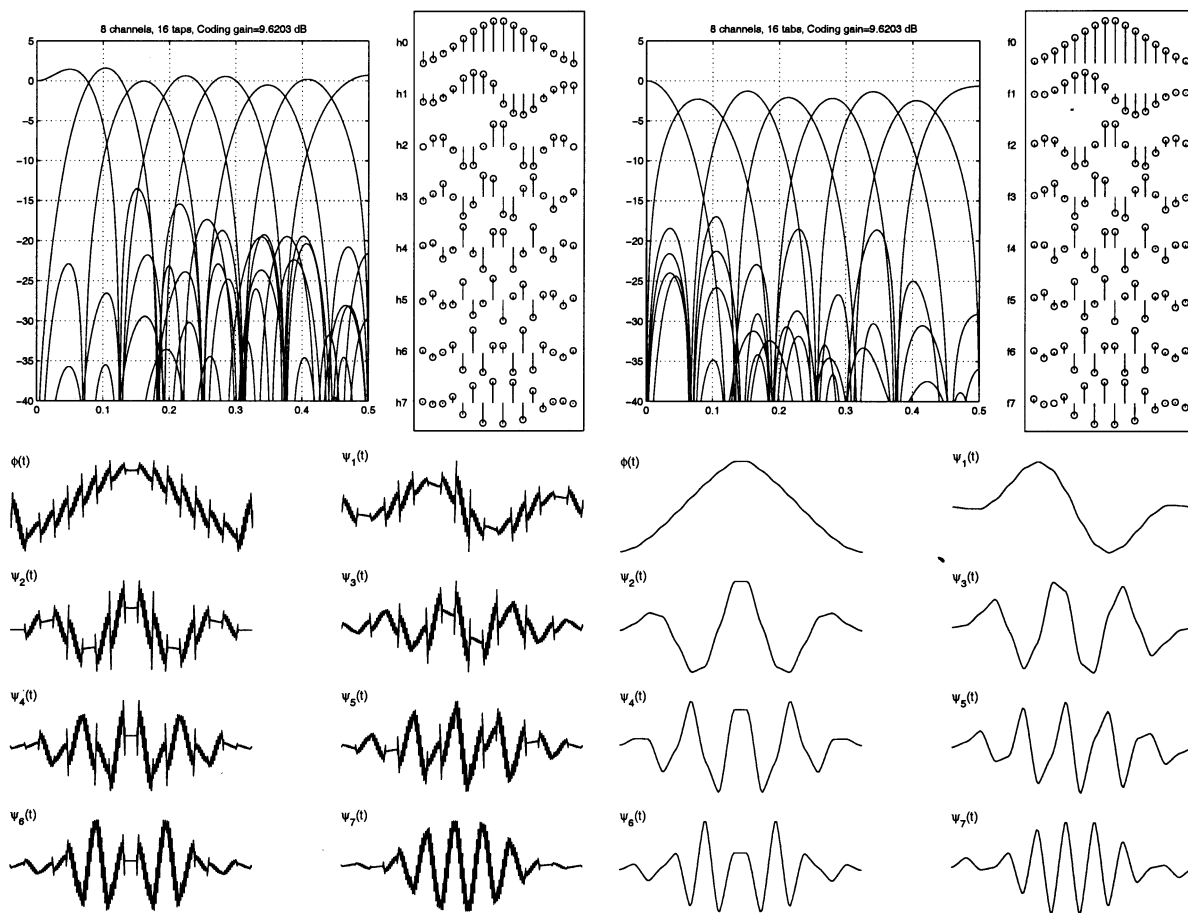


Fig. 5. Design example of (1, 1)-regular eight-channel BOLD filterbank with length 16. (Top left) Frequency responses of the analysis and (top right) synthesis filters and (bottom left) scaling function and wavelets of the analysis and (bottom right) synthesis banks.

have the same number of zeros at dc. In fact, this is equivalent to imposing the same number of zeros at mirror frequencies of the synthesis lowpass filter.

Condition A_{01} requires the analysis bandpass and highpass filters to have zero response at dc, i.e., $F_0(z)$ has regularity of degree one. This condition can be satisfied by constraining the sum of the elements in each row of \mathbf{U}_0 , except for the first one, to be zero. Similarly, condition A_{10} is equivalent to the fact that the synthesis bandpass and highpass filters have zero responses at dc, i.e., $H_0(z)$ is 1-regular. It is easy to show that conditions A_{01} and A_{10} together imply that $c_0 d_0 = L$. Therefore, in order to satisfy both conditions, all elements of the first row of \mathbf{U}_0 must be c_0/L . This is consistent with the result in the PU case, where $\mathbf{U}_0^{-T} = \mathbf{U}_0$; hence, $L/c_0 = c_0$, implying that $c_0 = \sqrt{L}$. In the case of BOLD filterbanks, if the first row of the matrix is a constant vector, the sum of the elements in each other row is zero as it is orthogonal to the first row. Therefore, only one of the two conditions is required to enforce the first degree of regularity in both analysis and synthesis bank, provided that $d_0 = L/c_0$.

Let \mathbf{U}_0 be parameterized as the matrix \mathbf{A} in Fig. 4, i.e., $\mathbf{U}_0 = \mathbf{RDLP}$, where now, $\bar{\mathbf{U}}_0$ denotes the submatrix $\bar{\mathbf{A}}$ in Fig. 4. Since $\mathbf{P}\mathbf{1}_L = \mathbf{1}_L$, it is easy to see that the first vanishing moment of the analysis and synthesis bandpass/highpass filters does not depend on the choice of \mathbf{P} .

Theorem 2: The conditions A_{01} and A_{10} can be simultaneously satisfied by choosing

$$\ell_1 = \ell_2 = \dots = \ell_{L-1} = -1, \quad \alpha = c_0 \quad \text{and} \\ \mathbf{r} = \frac{c_0}{L} \bar{\mathbf{U}}_0^{-T} \mathbf{1}_{L-1}$$

where $\mathbf{r} = [r_1 \ r_2 \ \dots \ r_{L-1}]^T$.

Note that the above conditions can be realized by any choice of $\bar{\mathbf{U}}_0$ as long as it is nonsingular, and $c_0 \neq 0$.

Proof: When all analysis bandpass and highpass filters have zero magnitude response at dc, we have $\mathbf{U}_0 \mathbf{1}_L = \mathbf{RDLP}\mathbf{1}_L = \mathbf{RDL}\mathbf{1}_L = c_0 \mathbf{a}_L$. Hence, $\mathbf{L}\mathbf{1}_L = c_0 \mathbf{D}^{-1} \mathbf{R}^{-1} \mathbf{a}_L = c_0 \mathbf{D}^{-1} \mathbf{a}_L = (c_0/\alpha) \mathbf{a}_L$, which implies that $\alpha = c_0$ and $\ell_i = -1$. Now, let us assume that the synthesis bandpass and highpass filters also have zero magnitude response at dc, i.e., $\mathbf{U}_0^{-T} \mathbf{1}_L = \mathbf{R}^{-T} \mathbf{D}^{-T} \mathbf{L}^{-T} \mathbf{P}\mathbf{1}_L = \mathbf{R}^{-T} \mathbf{D}^{-T} \mathbf{L}^{-T} \mathbf{1}_L = d_0 \mathbf{a}_L$. Therefore

$$d_0 \mathbf{R}^T \mathbf{a}_L = \mathbf{D}^{-T} \mathbf{L}^{-T} \mathbf{1}_L = \mathbf{D}^{-T} \begin{bmatrix} L \\ \mathbf{1}_{L-1} \end{bmatrix} \\ = d_0 \begin{bmatrix} 1 \\ \mathbf{r} \end{bmatrix} = \begin{bmatrix} L/\alpha \\ \bar{\mathbf{U}}_0^{-T} \mathbf{1}_{L-1} \end{bmatrix}$$

leading to $d_0 = L/\alpha = L/c_0$, and $\mathbf{r} = (1/d_0) \bar{\mathbf{U}}_0^{-T} \mathbf{1}_{L-1} = (c_0/L) \bar{\mathbf{U}}_0^{-T} \mathbf{1}_{L-1}$. \square

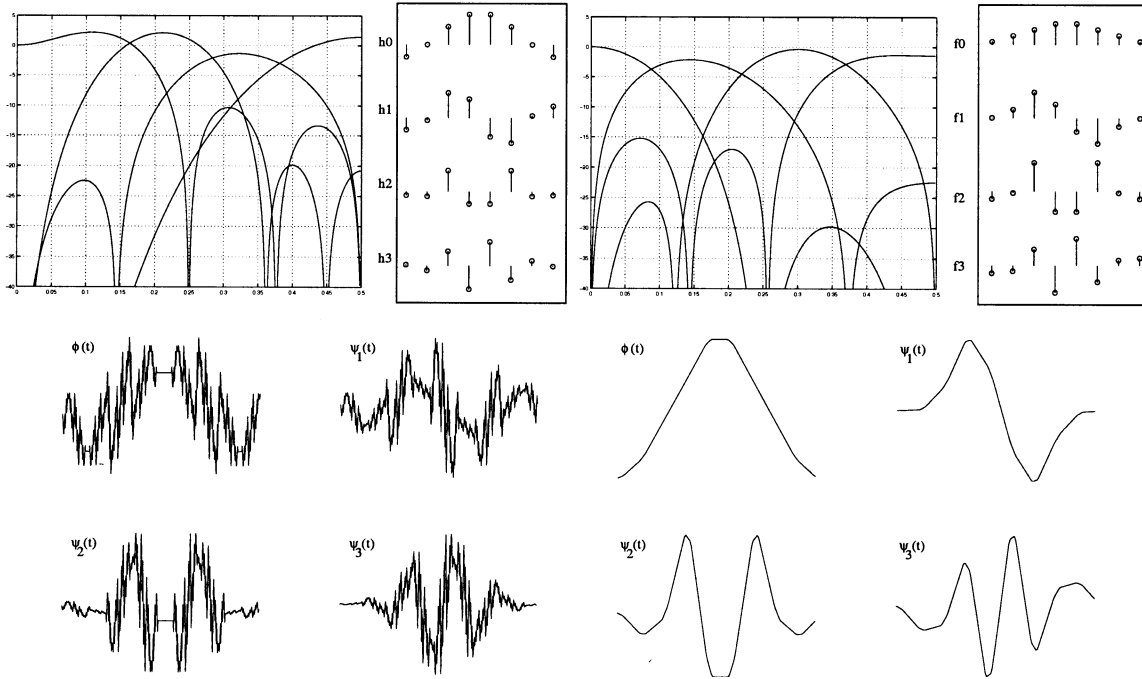


Fig. 6. Design example of (1, 2)-regular four-channel BOLP filterbank with length 8. (Top-left) Frequency and time responses of the analysis filters. (Top right) Frequency and time responses of the synthesis filters. (Bottom left) scaling function and wavelets of the analysis. (Bottom-right) Synthesis banks.

Example 1: In this paper, the filters in all design examples are optimized in order to maximize the stopband attenuation and coding gain, which can be given by

$$C_{\text{stopband attn.}} = - \sum_{i=0}^{M-1} \int_{\Omega_i} W_i(e^{j\omega}) |H_i(e^{j\omega})|^2 d\omega$$

$$C_{\text{coding gain}} = - \frac{10}{M} \log_{10} \prod_{i=0}^{M-1} \left(\sum_{m,n} h_i(n) h_i(m) \rho^{|m-n|} \right)$$

where ρ is the AR(1) correlation factor. In this paper, ρ is set to 0.95. In this design example, a (1, 1)-regular 16-tap eight-channel BOLP filterbank is designed using the proposed theory. The frequency responses, the zeros of the lowpass filters, and the corresponding scaling and wavelet functions of both analysis and synthesis bank are shown in Fig. 5.

B. (1, 2)-Regular Systems

We can follow the method in the previous case, assuming that both $H_0(z)$ and $F_0(z)$ have at least one regularity, i.e., the conditions A_{01} and A_{10} are satisfied. To obtain a (1, 2)-regular system, we have to impose another degree of regularity into $F_0(z)$. This is equivalent to the analysis bandpass and highpass filters having two zeros at dc (second vanishing moment). In terms of the lattice components, this is condition A_{02} . Note that this condition is exactly the same as that in the PU case [13], except that here, the matrices \mathbf{U}_0 and \mathbf{V}_i are nonsingular, and the condition A_{02} does not imply a second vanishing moment for the synthesis bank.

For convenience, let

$$\mathbf{c} = -c_0 \left(\mathbf{I} + \sum_{j=3}^{N-1} \prod_{i=N-3}^{N-j} \mathbf{V}_i \right) \mathbf{a}_L - \left(\prod_{i=N-3}^0 \mathbf{V}_i \right) \mathbf{b}_L.$$

Hence, the condition A_{02} can be simplified to

$$\mathbf{V}_{N-2} \mathbf{c} = c_0 \mathbf{a}_L. \quad (5)$$

Assuming that \mathbf{V}_i for $i < N-2$ are known, \mathbf{c} is also known. Let us parameterize \mathbf{V}_{N-2} as matrix \mathbf{A} in Fig. 4. Condition (5) can be satisfied by choosing the lifting parameters ℓ_i and α in Fig. 4, as in the following theorem.

Theorem 3: Let $\tilde{\mathbf{c}} = \mathbf{P}\mathbf{c}$. \mathbf{V}_{N-2} satisfies (5) if and only if

$$\alpha = \frac{c_0}{\tilde{c}_1} \quad \text{and} \quad \ell_i = -\frac{\tilde{c}_{i+1}}{\tilde{c}_1}, \quad \text{for } i = 1, \dots, L-1$$

where $\tilde{\mathbf{c}} = [\tilde{c}_1 \ \tilde{c}_2 \ \dots \ \tilde{c}_{L-1}]^T$.

Proof: Assume that (5) holds; therefore, we have $\mathbf{V}_{N-2} \mathbf{c} = \mathbf{RDL}\mathbf{P}\mathbf{c} = \mathbf{RDL}\tilde{\mathbf{c}} = \sqrt{L}\mathbf{a}_L$. Hence

$$\begin{aligned} & [\tilde{c}_1 \ \tilde{c}_2 + \ell_1 \tilde{c}_1 \ \tilde{c}_3 + \ell_2 \tilde{c}_1 \ \dots \ \tilde{c}_L + \ell_{L-1} \tilde{c}_1]^T \\ &= \mathbf{L}\tilde{\mathbf{c}} = \sqrt{L}\mathbf{D}^{-1}\mathbf{R}^{-1}\mathbf{a}_L \\ &= \sqrt{L}\mathbf{D}^{-1}\mathbf{a}_L = \alpha\sqrt{L}\mathbf{a}_L \end{aligned}$$

which completes the proof. \square

Example 2: In this design example, a (1, 2)-regular 16-tap, eight-channel BOLP filterbank is designed using the proposed theory.

C. (2, 2)-Regular Systems

In this section, we impose the second vanishing moment into both analysis and synthesis filterbanks. To begin, recall that the

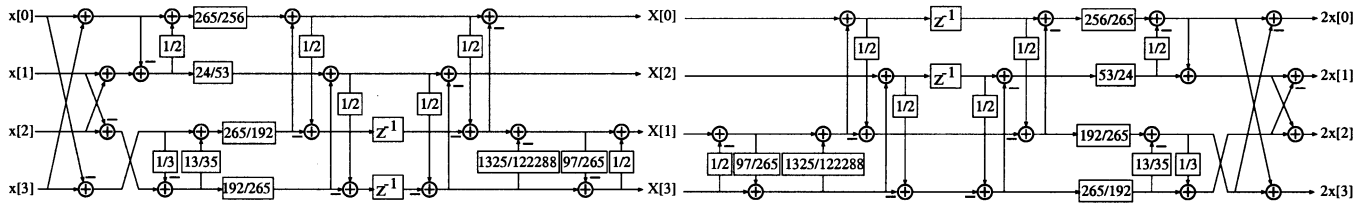


Fig. 7. Lattice structure of the (1, 2)-regular four-channel eight-tap rational-coefficient design example shown in Fig. 6. (Left) Analysis bank. (Right) Synthesis bank.

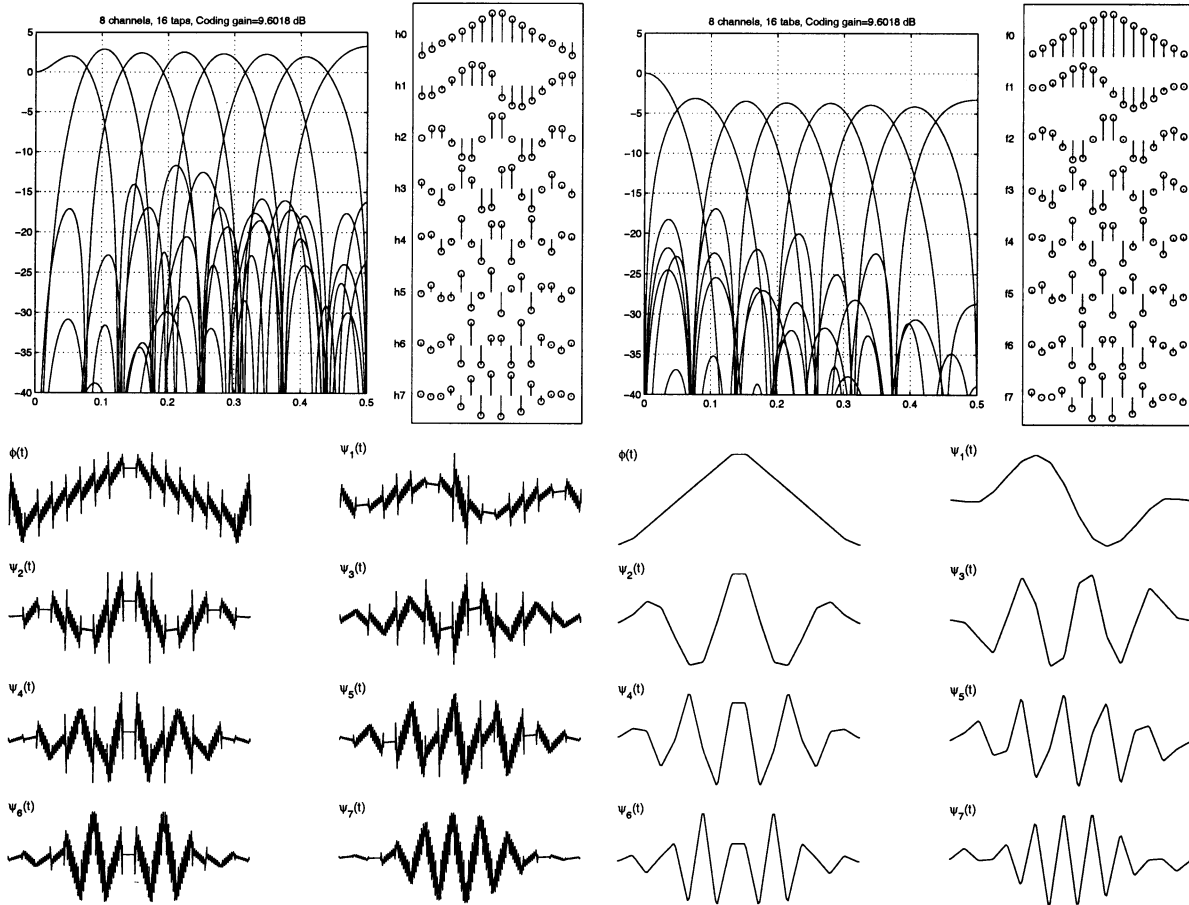


Fig. 8. Design example of (1, 2)-regular eight-channel BOLP filterbank with length 16. (Top left) Frequency responses of the analysis and (top right) synthesis filters. (Bottom left) Scaling function and wavelets of the analysis and (bottom right) synthesis banks.

filterbank is (2, 2)-regular; then, the condition A_{22} must be satisfied. Let

$$\mathbf{c} = -c_0 \left(\mathbf{I} + \sum_{j=3}^{N-1} \prod_{i=N-3}^{N-j} \mathbf{V}_i \right) \mathbf{a}_L + \left(\prod_{i=N-3}^0 \mathbf{V}_i \right) \mathbf{b}_L \quad (6)$$

$$\mathbf{d} = -\frac{L}{c_0} \left(\mathbf{I} + \frac{L}{c_0} \sum_{j=3}^{N-1} \prod_{i=N-3}^{N-j} \mathbf{V}_i^{-T} \right) \mathbf{a}_L + \left(\prod_{i=N-3}^0 \mathbf{V}_i^{-T} \right) \mathbf{b}_L. \quad (7)$$

The above conditions can be imposed into one of the $N - 1$ matrices $\mathbf{V}_i, i \leq N - 2$ if the other $N - 2$ matrices \mathbf{V}_i are known. Without loss of generality, let us assume that the matrices \mathbf{V}_i

are chosen in the increasing order. The above conditions can be rewritten as

$$\mathbf{V}_{N-2} \mathbf{c} = c_0 \mathbf{a}_L \quad (8)$$

$$\mathbf{V}_{N-2}^{-T} \mathbf{d} = \frac{L}{c_0} \mathbf{a}_L. \quad (9)$$

It is easy to show that both (8) and (9) hold only if

$$\mathbf{d}^T \mathbf{c} = (\mathbf{d}^T \mathbf{V}_{N-2}^{-1}) (\mathbf{V}_{N-2} \mathbf{c}) = \left(\frac{L}{c_0} \mathbf{a}^T \right) (c_0 \mathbf{a}) = L. \quad (10)$$

Clearly, this condition is independent of the choice of \mathbf{V}_i for $i \geq N - 2$. When $N = 2, \mathbf{c} = \mathbf{d} = \mathbf{b}_L$ and, hence, $\mathbf{d}^T \mathbf{c} = \|\mathbf{b}_L\|^2 \neq L$, which proves that the filter length of a (2, 2)-regular filterbank is at least $3M$ —a similar result to that of the PU case [22]. When $N \geq 3$, the above scalar algebraic equation can be imposed into one of the matrices \mathbf{V}_i with $i \leq N - 3$. Since the matrices \mathbf{V}_i are determined in increasing order, this condition

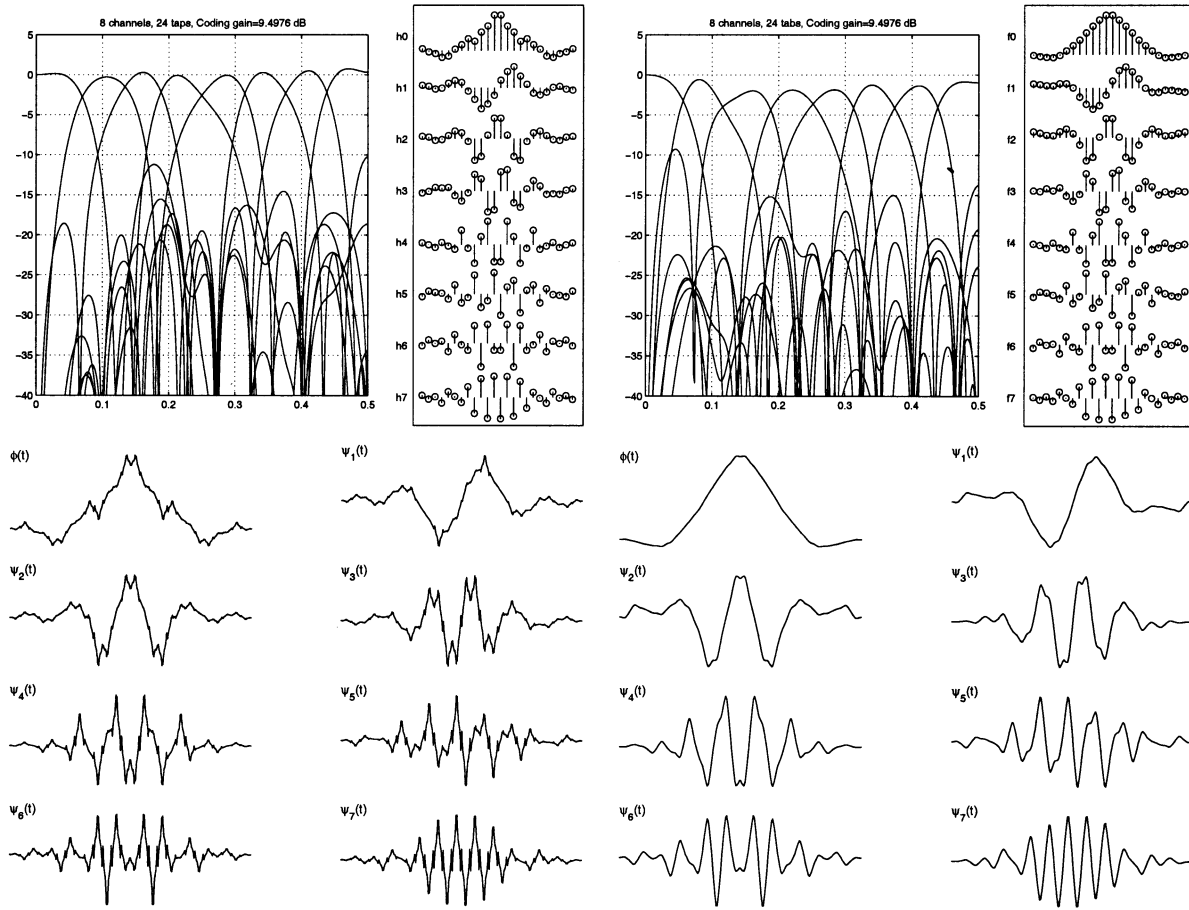


Fig. 9. Design example of (2, 2)-regular eight-channel BOLP filterbank with length 24. (Top left) Frequency responses of the analysis and (top right) synthesis filters. (Bottom left) Scaling function and wavelets of the analysis and (bottom right) synthesis banks.

can be imposed onto \mathbf{V}_{N-3} after \mathbf{V}_i for $i < N - 3$ are known. Let

$$\hat{\mathbf{c}} = -c_0 \left(\mathbf{I} + \sum_{j=4}^{N-1} \prod_{i=N-4}^{N-j} \mathbf{v}_i \right) \mathbf{a}_L + \left(\prod_{i=N-4}^0 \mathbf{v}_i \right) \mathbf{b}_L$$

and

$$\hat{\mathbf{d}} = -\frac{L}{c_0} \left(\mathbf{I} + \frac{L}{c_0} \sum_{j=4}^{N-1} \prod_{i=N-4}^{N-j} \mathbf{v}_i^{-T} \right) \mathbf{a}_L + \left(\prod_{i=N-4}^0 \mathbf{v}_i^{-T} \right) \mathbf{b}_L.$$

Then, (10) becomes

$$\frac{L}{c_0} \mathbf{a}_L^T \mathbf{V}_{N-3} \hat{\mathbf{c}} + c_0 \hat{\mathbf{d}}^T \mathbf{V}_{N-3}^{-T} \mathbf{a}_L + \hat{\mathbf{c}}^T \hat{\mathbf{d}} = 0. \quad (11)$$

Let \mathbf{V}_{N-3} be parameterized as matrix \mathbf{A} in Fig. 4. After some manipulation, one can show that (11) implies

$$\frac{L}{c_0} [\alpha + \mathbf{r}^T \tilde{\mathbf{V}}_{N-3} \mathbf{l} \mathbf{r}^T \tilde{\mathbf{V}}_{N-3}] \mathbf{P} \hat{\mathbf{c}} + \frac{c_0}{\alpha} \mathbf{d}^T \mathbf{P} \begin{bmatrix} 1 \\ 1 \end{bmatrix} + \hat{\mathbf{c}}^T \hat{\mathbf{d}} = 0. \quad (12)$$

It is easy to show that both (11) and (12) can be easily imposed onto one of the liftings r_i and ℓ_i of \mathbf{V}_{N-3} as it forms a linear

equation of each of these parameters. One can also impose this into α ; however, the equation becomes quadratic, and it is possible for α to be complex for some choices of r_i and ℓ_i .

Theorem 4: If \mathbf{U}_0 satisfies the conditions A_{01} and A_{10} and \mathbf{V}_{N-3} satisfies (11), for any choices of \mathbf{V}_i ($i < N - 2$), the resulting filterbank is (2, 2)-regular if and only if the following conditions hold:

- 1) $\alpha = \sqrt{L}/\tilde{c}_1$;
- 2) $\ell_i = -((\tilde{c}_{i+1})/\tilde{c}_1)$ for $i = 1, \dots, L - 1$;
- 3) $[r_1 \ r_2 \ \dots \ r_{L-1}] = (\alpha/\tilde{d}_1)[\tilde{d}_2 \ \tilde{d}_3 \ \dots \ \tilde{d}_L] \tilde{\mathbf{V}}_{N-2}^{-1}$;

where $\tilde{\mathbf{c}} = \mathbf{P}\mathbf{c}$, and $\tilde{\mathbf{d}} = \mathbf{P}\mathbf{d}$.

In the design process, the matrix \mathbf{V}_{N-2} can be parameterized as follows. The vectors \mathbf{c} and \mathbf{d} are obtained from (6) and (7). The only constraint before obtaining \mathbf{c} and \mathbf{d} is that \mathbf{V}_{N-3} must satisfy (11), which can easily be done by enforcing one of its parameter to satisfy (12). The vectors $\tilde{\mathbf{c}}$ and $\tilde{\mathbf{d}}$ are obtained after the permutation matrix \mathbf{P} has been identified, and finally, α , ℓ_i , and r_i are defined.

Proof: Conditions 1 and 2 are exactly the same as that in Theorem 3. From (9), we have

$$\begin{aligned} \mathbf{V}_{N-2}^{-T} \mathbf{d} &= \mathbf{R}^{-T} \mathbf{D}^{-T} \mathbf{L}^{-T} \mathbf{P} \mathbf{d} = \mathbf{R}^{-T} \mathbf{D}^{-T} \mathbf{L}^{-T} \tilde{\mathbf{d}} \\ &= \frac{L}{c_0} \mathbf{a}_L. \end{aligned}$$

TABLE I
OBJECTIVE PROPERTIES OF THE PULP FILTERBANKS USED IN IMAGE COMPRESSION EXPERIMENTS

Transform Prop- erty	8 × 8 DCT	8 × 16 LOT	8 × 24 PULPv1	8 × 24 PULPv2	8 × 16 BOLPv11	8 × 16 BOLPv12	8 × 24 BOLPv22
Coding gain (dB)	8.83	9.22	9.36	9.33	9.62	9.60	9.50
Deg. of regularity	1	1	1	2	(1,1)	(1,2)	(2,2)
Stopband attn.(dB)	4.43	16.32	19.48	13.00	13.76	12.53	9.93

TABLE II
OBJECTIVE CODING RESULTS (PSNR IN DECIBELS) USING DIFFERENT TRANSFORMS WITH ONE LEVEL DECOMPOSITION IN THE LOWPASS SUBBAND ON TEST IMAGES LENA AND BARBARA

Lena	PSNR (dB)							
Comp. ratio	(9,7) Wavelet	8 × 8 DCT	8 × 16 LOT	8 × 24 PULPv1	8 × 24 PULPv2	8 × 16 BOLPv11	8 × 16 BOLPv12	8 × 24 BOLPv22
1:8	40.41	39.91	40.05	40.36	40.21	40.35	40.20	40.19
1:16	37.21	36.38	36.72	37.16	36.90	37.28	37.07	36.98
1:32	34.11	32.90	33.56	33.97	33.61	34.14	33.97	33.89
1:64	31.10	29.67	30.48	30.80	30.48	31.04	30.86	30.88
1:100	29.35	27.80	28.62	28.93	28.72	29.14	28.99	29.14
1:128	28.38	26.91	27.61	27.95	27.79	28.20	28.01	28.16
Barbara	PSNR (dB)							
Comp. ratio	(9,7) Wavelet	8 × 8 DCT	8 × 16 LOT	8 × 24 PULPv1	8 × 24 PULPv2	8 × 16 BOLPv11	8 × 16 BOLPv12	8 × 24 BOLPv22
1:8	36.41	36.31	37.43	37.95	37.45	37.84	37.64	37.22
1:16	31.40	31.11	32.70	33.07	32.61	33.02	32.74	32.48
1:32	27.58	27.28	28.80	29.06	28.76	29.04	28.80	28.74
1:64	24.86	24.58	25.70	25.91	25.78	26.00	25.94	25.84
1:100	23.76	23.42	24.34	24.59	24.55	24.55	24.38	24.52
1:128	23.35	22.68	23.37	23.62	23.68	23.49	23.80	23.89

Hence

$$\begin{aligned} \frac{L}{c_0} \mathbf{R}^T \mathbf{a}_L &= \frac{L}{c_0} [1 \quad r_1 \quad \cdots \quad r_{L-1}]^T \\ &= \left[\tilde{\mathbf{V}}_{N-2}^{-T} [\tilde{d}_2 \quad \tilde{d}_3 \quad \cdots \quad \tilde{d}_L]^T \right] \end{aligned}$$

for some β . It is easy to show that with the choice of \mathbf{V}_{N-3} in (12), $\beta = L/c_0$, and thus, the proof is complete. \square

Since the construction of (2, 2)-regular filterbanks is quite complicated, we summarize all the parameterizing steps here.

- 1) Parameterize \mathbf{U}_0 to satisfy the conditions A_{01} and A_{10} .
 - 1.1) Choose any $\tilde{\mathbf{U}}_0$.
 - 1.2) Choose ℓ_i, r_i , and α of \mathbf{U}_0 , as in Theorem 4, where \mathbf{P} is a permutation matrix, as described in Section IV.
- 2) Choose \mathbf{V}_i for $0 \leq i \leq N-4$ arbitrarily if $N \geq 4$.
- 3) Parameterize \mathbf{V}_{N-3} to satisfy (11) by choosing ℓ_i and r_i of \mathbf{V}_{N-3} that satisfy (12).
- 4) Choose ℓ_i, r_i , and α of \mathbf{V}_{N-2} , as in Theorem 4, where \mathbf{P} is a permutation matrix, as described in Section IV.
- 5) Choose \mathbf{V}_{N-1} arbitrarily.

Example 3: In this design example, a (2, 2)-regular 24-tap eight-channel BOLP filterbank is designed using the proposed theory.

It should be noted that in Examples 1 and 3, even though the degree of regularity of the analysis and synthesis filters are

equal, optimization of coding gain can still automatically force unsymmetrical smoothness of the resulting analysis and synthesis scaling functions. This is consistent with one of our objectives that the synthesis basis function should be smooth, whereas the analysis one should decorrelate the input signal, and thus, smoothness is not critically important.

D. Regular Filterbanks With Rational Coefficients

One advantage of the proposed parameterization is that the lifting scheme is used, and thus, rational coefficients can be obtained while perfect reconstruction is preserved. See [23] for a detailed discussion on how to design such a class of filterbank.

Example 4: In this design example, a (1, 2)-regular eight-tap four-channel BOLP filterbank is designed using the proposed theory. The frequency responses, the time responses, and the corresponding scaling and wavelet functions of both analysis and synthesis banks are shown in Fig. 6, where the enhanced smoothness in the synthesis bank is evident. Note that we purposely choose rational parameters in this design. The detailed rational-coefficient lattice is depicted in Fig. 7. The frequency responses, the zeros of the lowpass filters, and the corresponding scaling and wavelet functions of the analysis and synthesis banks of Example 2 are shown in Fig. 8. The frequency responses, the zeros of the lowpass filters, and the corresponding scaling and wavelet functions of the analysis and synthesis banks of Example 3 are shown in Fig. 9.

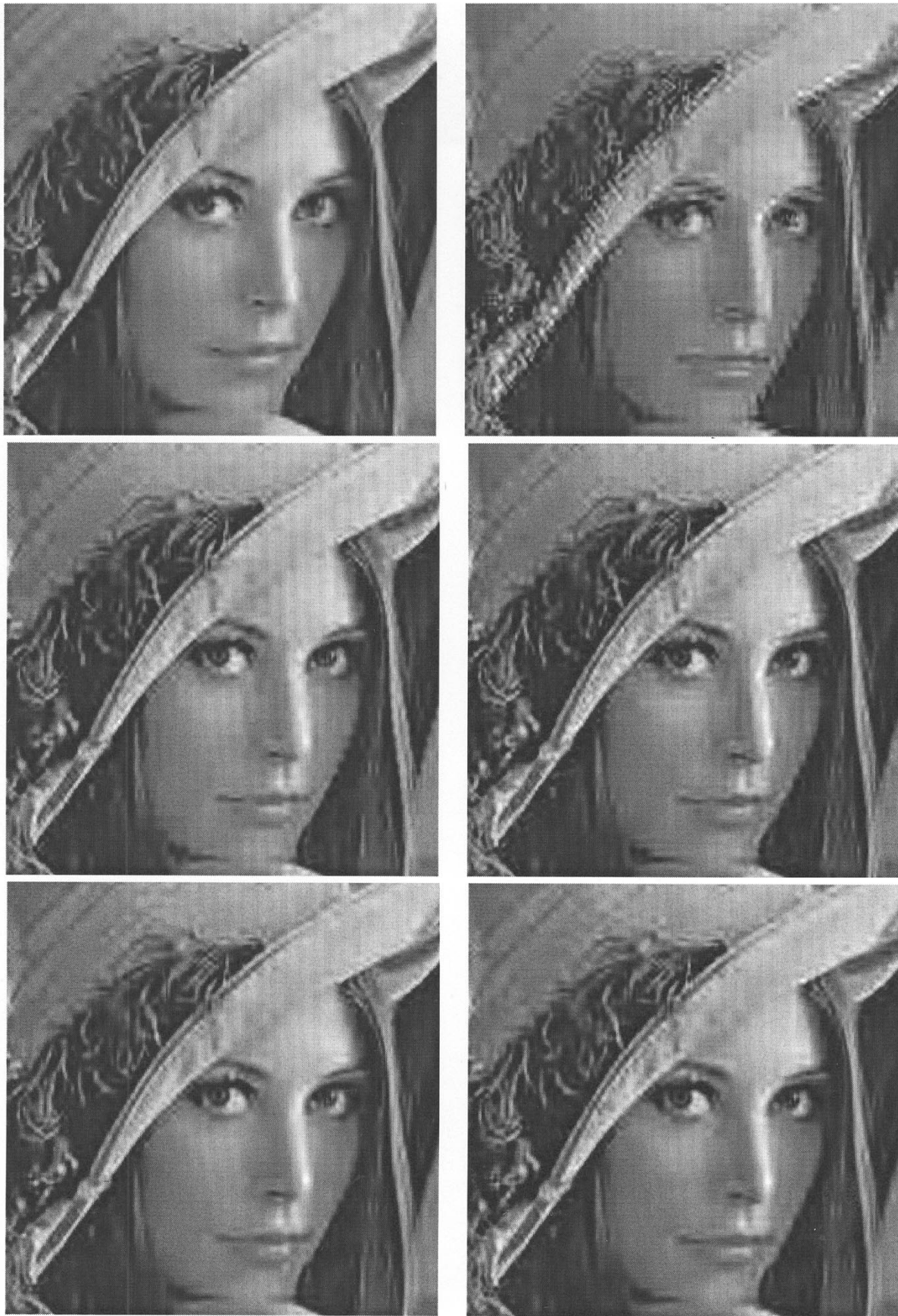


Fig. 10. Enlarged portions of the Lena image compressed at 1:64 using various linear phase filterbanks. (Top left) 9/7 wavelet. (Top right) 8×16 LOT (top-right). (Middle left) 8×24 1-regular PULP filterbank. (Middle right) 8×24 2-regular PULP filterbank. (Bottom left) 8×16 (1, 1)-regular BOLP filterbank. (Bottom right) 8×16 (1, 2)-regular BOLP filterbank.



Fig. 11. Enlarged portions of the Barbara image compressed at 1:64 using various linear-phase filterbanks. (Top left) 9/7 wavelet. (Top right) 8×16 LOT. (Middle left) 8×24 1-regular PULP filterbank. (Middle right) 8×24 2-regular PULP filterbank. (Bottom left) 8×16 (1, 1)-regular BOLP filterbank. (Bottom right) 8×16 (1, 2)-regular BOLP filterbank.

TABLE III
OBJECTIVE CODING RESULTS (PSNR IN DECIBELS) USING DIFFERENT TRANSFORMS WITH TWO LEVEL DECOMPOSITION IN THE LOWPASS SUBBAND ON TEST IMAGES LENA AND BARBARA

Lena	PSNR (dB)							
Comp. ratio	(9/7) Wavelet	8 × 8 DCT	8 × 16 LOT	8 × 24 PULPv1	8 × 24 PULPv2	8 × 16 BOLPv11	8 × 16 BOLPv12	8 × 24 BOLPv22
1:8	40.41	39.88	40.02	40.33	40.18	40.33	40.20	40.16
1:16	37.21	36.31	36.67	37.10	36.84	37.24	37.05	36.91
1:32	34.11	32.77	33.45	33.86	33.48	34.03	33.85	33.74
1:64	31.10	29.45	30.29	30.66	30.30	30.85	30.64	30.63
1:100	29.35	27.55	28.32	28.68	28.45	28.89	28.78	28.82
1:128	28.38	26.68	27.37	27.74	27.55	27.93	27.77	27.86
Barbara	PSNR (dB)							
Comp. ratio	(9/7) Wavelet	8 × 8 DCT	8 × 16 LOT	8 × 24 PULPv1	8 × 24 PULPv2	8 × 16 BOLPv11	8 × 16 BOLPv12	8 × 24 BOLPv22
1:8	36.41	36.29	37.40	37.92	37.41	37.81	37.57	37.17
1:16	31.40	31.07	32.66	33.04	32.55	32.97	32.73	32.40
1:32	27.58	27.21	28.72	28.99	28.65	28.95	28.81	28.62
1:64	24.86	24.48	25.58	25.81	25.65	25.89	25.78	25.58
1:100	23.76	23.33	24.23	24.48	24.43	24.33	24.44	24.41
1:128	23.35	22.53	23.22	23.48	23.52	23.46	23.42	23.71

V. CODING EXAMPLES

In this section, the regular filterbanks obtained from several design examples presented in previous sections are evaluated in an image compression application. The test images in the experiment are popular 512×512 8-bit gray-scale images *Lena* and *Barbara*, representing images with smooth regions and textures respectively. The set partitioning in hierarchical trees (SPIHT) progressive image transmission algorithm is chosen to compare the performances of the transforms, i.e., the encoding algorithm is fixed and only the decomposition stage in the encoder, and the reconstruction stage in the decoder is modified with different transformations. The eight transforms chosen for the experiment are the following:

- two-band 9/7 Daubechies symmetric wavelets [24], four degrees of regularity, six levels of iteration;
- eight-band eight-tap DCT [8], one degree of regularity, two levels of iteration;
- eight-band 16-tap LOT [5], one degree of regularity, two levels of iteration;
- eight-band 24-tap PULP regular FB labeled PULPv1 [13], one degree of regularity, two levels of iteration;
- eight-band 24-tap PULP regular FB labeled PULPv2 [13], two degrees of regularity, two levels of iteration;
- eight-band 16-tap BOLP regular FB labeled BOLPv11, (1, 1)-degree of regularity, two levels of iteration;
- eight-band 16-tap BOLP regular FB labeled BOLPv12, (1, 2)-degree of regularity, two levels of iteration;
- eight-band 24-tap BOLP regular FB labeled BOLPv22, (2, 2)-degree of regularity, two levels of iteration.

Table I summarizes the coding gains, degrees of regularity, and stopband attenuation of the M -band transforms used in the comparison. To avoid modification of the encoding algorithm, the transform coefficients are rearranged and grouped into the popular quad-tree structure [25], [26]. Thus, an eight-band filterbank is equivalent to a three-level dyadic wavelet iteration.

Table II summarizes the PSNR of the reconstruction images. According to Table II, for *Lena*, the (9/7)-wavelet yields highest PSNRs for most of the compression ratios except for 1:16 and 1:32, where the BOLPv11 is better. Comparing among the eight-channel filterbanks, both the BOLPv11 and BOLPv12 yield approximately equal PSNRs to that of the PULPv1 and PULPv2, despite their shorter filter length. However, the reconstructions have different perceptual quality. Fig. 10 shows an enlarged portion of the *Lena* image coded using different filterbanks at a 1:64 compression ratio. It is clear that the blocking artifact appearing in the case of the LOT is improved by the PULPv1 and PULPv2 and completely eliminated by the BOLPv11 and BOLPv12. In addition, the biorthogonal transforms seem to preserve the fine details better than the orthogonal ones. In this case, since the *Lena* image has a lot of smooth regions, as expected, the 9/7 wavelet yields highest PSNR and perceptually similar reconstruction to that of the BOLPv12. A similar case but with richer textures is found in the second test image. Fig. 11 depicts the enlarged portion of the *Barbara* image coded at 1:64 compression ratio. It is clear that in the orthogonal cases (LOT, PULPv1, and PULPv2), not only is there residual blocking artifact in the reconstruction but also, some of the texture details are lost. These textures are better preserved by the biorthogonal transforms (BOLPv11 and BOLPv12). In this case, since the *Barbara* image has a lot of textures, the 9/7 wavelet smoothes out many high-frequency details.

In order to obtain a fair comparison to the coding results in [13], the lowpass subband of the eight-channel filterbank is fed to another stage of transformation. This two-level decomposition of the eight-channel filterbank is equivalent to a six-level dyadic wavelet transform after the coefficients are rearranged. Table III presents the resulting coding PSNRs. Compared with Table II, the new PSNRs are similar to that when the filterbanks are not reiterated but slightly lower. The differences are uniform across the transforms, i.e., at each compression ratio, the degradations in PSNRs are approximately the same for different eight-

channel filterbanks. This suggests that when an M -channel filterbank with sufficiently large M is used, there is no need for re-iteration in the lowpass branch as that used in the dyadic case.

VI. CONCLUSION

In this paper, we have presented a method for imposing regularity properties onto BOLP filterbanks. A new lattice structure for parameterizing a nonsingular matrix via lifting steps is presented. This new structure has several advantages over the conventional direct and SVD parameterizations in terms of number of free parameters and robustness to the quantization of the lifting coefficients. Regarding regular filterbanks, we consider three cases of (1, 1), (1, 2), and (2, 2)-regular systems, where the corresponding permissible minimal filter lengths are M , $2M$, and $3M$, respectively. By using the proposed parameterization of nonsingular matrices, the conditions for regularity of the filterbanks can be imposed with ease into the lifting steps. Finally, these transforms are tested in an image coding application and shown to simultaneously eliminate the blocking artifact and preserve texture details better than the conventional transforms.

APPENDIX

PROOF OF PROPOSITION 1

- 1) We will prove, by using the modulation matrices $\mathbf{H}_m(z)$ and $\mathbf{F}_m(z)$, whose (i, j) elements are $H_i(W^j)$ and $F_i(W^j)$, where $W = e^{j2\pi/M}$. First, let us prove the first statement by induction on K_s . Recall that the PR property of the filterbank yields

$$\mathbf{F}_m(z)\mathbf{H}_m^T(z) = \text{a diagonal matrix.} \quad (13)$$

- a) $\underline{K_s = 1}$. Assume that $F_0(W^j) = 0$ for all $j = 1, 2, \dots, M-1$. Substituting $z = 1$ into (13) yields

$$\sum_j F_0(W^j z) H_j(W^j z) = 0$$

for all $i > 0$. Hence, $H_i(1) = 0$.

- b) $\underline{K_s = n}$. Assume that the first statement of the theorem is true for $K_s < n$. It is now sufficient to show that if $F_0(z)$ has n multiple zeros at aliasing frequencies W^j for all $j > 0$, then $H_i(z)$ have n multiple zeros at dc frequency. Suppose that $F_0(z)$ has n zeros at W^j for all $j > 0$ in order to show that the bandpass/highpass filters $H_i(z)$ have n zeros at dc for all $i > 0$, and it suffices to show that $H_i(z)$ are of the form $H_i(z) = (1 - z^{-1})^n Q_i(z)$, where $Q_i(z)$ are some polynomials (since all the filters are FIR) in z^{-1} . Equivalently, the r th derivative of $H_i(z)$ with respect to z^{-1} and evaluated at $z = 1$ is zero for all $r = 0, 1, \dots, n-1$. Repeatedly applying the derivative operator $n-1$ times to (13) with respect to z^{-1} implies that

$$\sum_{\ell=0}^{n-1} \binom{n-1}{\ell} [\mathbf{F}_m(z)]^{(\ell)} [\mathbf{H}_m^T(z)]^{(n-1-\ell)} = \text{diagonal matrix.} \quad (14)$$

After substituting $z = 1$, we can rewrite (14) as

$$\begin{aligned} & [\mathbf{F}_m(z)] [\mathbf{H}_m^T(z)]^{(n-1)} \Big|_{z=1} + \sum_{\ell=1}^{n-1} \binom{n-1}{\ell} [\mathbf{F}_m(z)]^{(\ell)} \\ & \times [\mathbf{H}_m^T(z)]^{(n-1-\ell)} \Big|_{z=1} = \text{diagonal matrix.} \quad (15) \end{aligned}$$

Consider the off-diagonal elements of the first column of $[\mathbf{F}_m(z)]^{(\ell)} [\mathbf{H}_m^T(z)]^{(n-1-\ell)} \Big|_{z=1}$. Since $F_0(z)$ has n zeros at all aliasing frequencies, the off-diagonal elements of the first row in $[\mathbf{F}_m(z)]^{(\ell)} \Big|_{z=1}$ are zero for $\ell = 0, 1, \dots, n-1$. By the assumption of induction, the off-diagonal elements of the first row in $[\mathbf{H}_m(z)]^{(n-1-\ell)} \Big|_{z=1}$ are zero for $\ell = 1, 2, \dots, n-1$, which imply that the off-diagonal elements of the first row in $[\mathbf{F}_m(z)] [\mathbf{H}_m^T(z)]^{(n-1)} \Big|_{z=1}$ must be zero, i.e.,

$$\sum_j [F_0(W^j z)] [H_k(W^j z)]^{(n-1)} \Big|_{z=1} = 0 \quad (16)$$

for $k = 1, 2, \dots, M$. Hence, $[H_k(z)]^{(n-1)} \Big|_{z=1} = 0$ for all $k > 0$, which completes the proof. The second statement can be proven in the same manner by noting that

$$\mathbf{F}_m^T(z)\mathbf{H}_m(z) = \text{diagonal matrix} \quad (17)$$

and will be left as a simple exercise for the reader.

- 2) We will show only for the case of (a) since the two conditions are analogous. The proof is straightforward from the fact that $H_i(z)$ has K_s zeros at dc. Let us write $H_i(z)$ as

$$H_i(z) = \sum_n h_i(n) z^{-n} = (z-1)^{K_s} Q^0(z) \quad (18)$$

where $Q^0(z)$ is some function of z such that $Q^0(1) \neq 0$. Hence, $\sum_n h_i(n) = H_i(1) = 0$. Now, letting us differentiate (18) with respect to z , we get

$$\begin{aligned} - \sum_n n h_i(n) z^{-n-1} &= (z-1)^{K_s-1} \\ &\times \left[K_s Q^0(z) + (z-1) \frac{d}{dz} Q^0(z) \right]. \end{aligned}$$

Letting $Q^1(z) = -z[K_s Q^0(z) + (z-1)(d/(dz))Q^0(z)]$, then

$$\sum_n n h_i(n) z^{-n} = (z-1)^{K_s-1} Q^1(z). \quad (19)$$

It is clear that if $K_s > 1$, substituting $z = 1$ into (19) implies (a) for $n = 1$. For $n = 2, \dots, K_s$, successively differentiating and substituting $z = 1$, as above, completes the proof.

- 3) We will only prove for $\psi_i(t)$. From the definition of $\psi_i(t)$ for $i > 0$, we have

$$\begin{aligned}
& \int t^j \psi_i(t) dt \\
&= \int t^j \sum_k h_i(k) \phi(Mt - k) dt \\
&= \int \sum_k t^j h_i(k) \phi(Mt - k) dt \\
&= \int \sum_k \left(\frac{\tau + k}{M}\right)^j h_i(k) \phi(\tau) \frac{d\tau}{M} \\
&= \frac{1}{M^{j+1}} \int \phi(\tau) \sum_k \sum_{\ell=0}^j \binom{j}{\ell} \tau^{j-\ell} k^\ell h_i(k) d\tau \\
&= \frac{1}{M^{j+1}} \int \phi(\tau) \sum_{\ell=0}^j \binom{j}{\ell} \tau^{j-\ell} \sum_k k^\ell h_i(k) d\tau.
\end{aligned}$$

From 2, if $j \leq K_s$, the ℓ th moment of $h_i(k)$ in the last equation is zero because $\ell \leq j \leq K_s$, and hence, $\int t^j \psi_i(t) dt = 0$, as desired.

- 4) We will integrate by part the quantity in the absolute value. Let $I^1(t) = \int_{-\infty}^t \tilde{\psi}_i(\tau) d\tau$; hence, $\tilde{\psi}_i(M^j t - k) dt = M^{-j} dI^1(M^j t - k)$. From 3, it is clear that $I^1(\infty) = 0$. In fact, $I^1(t)$ has the same compact support as $\tilde{\psi}_i(t)$. Therefore

$$\int g(t) \tilde{\psi}_i(M^j t - k) dt = -M^{-j} \int g'(t) I^1(M^j t - k) dt. \quad (20)$$

Again, let $I^2(t) = \int_{-\infty}^t I^1(\tau) d\tau = \int_{-\infty}^t \int_{-\infty}^{\tau} \tilde{\psi}_i(s) ds d\tau$. Integrating by parts, the above equation yields

$$\begin{aligned}
I^2(t) &= \tau I^1(\tau) \Big|_{-\infty}^t - \int_{-\infty}^t \tau dI^1(\tau) \\
&= \tau I^1(\tau) \Big|_{-\infty}^t - \int_{-\infty}^t \tau \tilde{\psi}_i(\tau) d\tau.
\end{aligned}$$

Hence, $I^2(\infty) = 0$, and (20) becomes

$$\int g(t) \tilde{\psi}_i(M^j t - k) dt = M^{-2j} \int g''(t) I^2(M^j t - k) dt. \quad (21)$$

Repeating the same procedure yields

$$\begin{aligned}
& \left| \int g(t) \tilde{\psi}_i(M^j t - k) dt \right| \\
&= \left| M^{-jK_s} \int g^{(K_s)}(t) I^{K_s}(M^j t - k) dt \right| \\
&\leq CM^{-jK_s} \|g^{(K_s)}(t)\|. \quad (22)
\end{aligned}$$

- 5) The proof is directly from the orthogonality between $\phi(t)$ and $\tilde{\psi}_i(t)$.
- 6) We will prove by induction on K_a , similar to the case of $M = 2$ in [1]. Let $\hat{\mathbf{L}}$ be the $M \times M$ submatrix of \mathbf{L} . Hence, the eigenvalues of $\hat{\mathbf{L}}$ are also eigenvalues of \mathbf{L} . When $K_s = 1$, $H_0(z)$ has a factor $(1 + z^{-1} + \dots + z^{1-M})$, which implies that $\sum_k h_0(Mk + j) = 1/M$ for all j . Hence, we have the equation at the bottom of the page. Therefore, 1 is an eigenvalue of $\hat{\mathbf{L}}$ and \mathbf{L} with the corresponding left eigenvector $[1 \ 1 \ \dots \ 1]$. Now, assuming that $H_0(z) = ((1 + z^{-1} + \dots + z^{1-M})/M)H_{\text{old}}(z)$, with $H_{\text{old}}(z)$ having $K_a = N$ zeros at every aliasing frequency $(2\pi k)/M$, let $\hat{\mathbf{L}}_{\text{old}} \mathbf{x}_{\text{old}} = \lambda_{\text{old}} \mathbf{x}_{\text{old}}$, where the equivalent relation can be expressed in the z -domain as

$$\begin{aligned}
& \sum_{k=0}^{M-1} H_{\text{old}}(W^k z) X_{\text{old}}(W^k z) = \lambda_{\text{old}} X_{\text{old}}(z^M). \\
& \left(\frac{1 - z^{-M}}{M}\right) \lambda_{\text{old}} X_{\text{old}}(z^M) \\
&= \left(\frac{1 - z^{-M}}{M}\right) \sum_{k=0}^{M-1} H_{\text{old}}(W^k z) X_{\text{old}}(W^k z) \\
&= \sum_{k=0}^{M-1} \left\{ \frac{1 + (W^k z)^{-1} + \dots + (W^k z)^{M-1}}{M} \right\} \\
&\quad \times H_{\text{old}}(W^k z) (1 - (W^k z)^{-1}) X_{\text{old}}(W^k z) \\
&= \sum_{k=0}^{M-1} H_0(W^k z) (1 - (W^k z)^{-1}) X(W^k z).
\end{aligned}$$

Hence, $\sum_{k=0}^{M-1} H_0(W^k z) X_{\text{new}}(W^k z) = (\lambda_{\text{old}}/M) X_{\text{new}}(z^M)$, where $X_{\text{new}}(z) = (1 - z^{-1})X_{\text{old}}(z)$, and thus, $\lambda_{\text{new}} = \lambda_{\text{old}}/M$ are new eigenvalues of \mathbf{L} . The extra eigenvalue 1 of \mathbf{L} follows from the fact that $\sum_k h_0(Mk + j) = 1/M$ for all j .

$$\begin{aligned}
& [1 \ 1 \ \dots \ 1] \hat{\mathbf{L}} = M [1 \ 1 \ \dots \ 1] \begin{bmatrix} h_0(0) & & & & & \\ h_0(M) & h_0(M-1) & h_0(M-2) & \dots & h_0(1) & h_0(0) \\ & h_0(2M-1) & h_0(2M-2) & \dots & h_0(M+1) & h_0(M) \\ & \vdots & \vdots & \vdots & \vdots & \vdots \\ & & & & & \vdots \end{bmatrix} \\
&= [1 \ 1 \ \dots \ 1].
\end{aligned}$$

REFERENCES

- [1] G. Strang and T. Nguyen, *Wavelets and Filter Banks*. Wellesley, MA: Wellesley-Cambridge, 1996.
- [2] K. R. Rao and J. J. Hwang, *Techniques and Standards for Image, Video, and Audio Coding*. Englewood Cliffs, NJ: Prentice-Hall, 1996.
- [3] *Wavelet Scalar Quantization Gray Scale Fingerprint Image Compression Specification*. Washington, DC: FBI Criminal Justice Information Services, 1993.
- [4] K. Sayood, *Introduction to Data Compression*. San Francisco, CA: Morgan Kaufmann, 2000.
- [5] H. S. Malvar, *Signal Processing with Lapped Transforms*. Norwood, MA: Artech House, 1992.
- [6] R. L. de Queiroz, T. Q. Nguyen, and K. R. Rao, "The genLot: Generalized linear-phase lapped orthogonal transform," *IEEE Trans. Signal Processing*, vol. 44, pp. 497–507, Mar. 1996.
- [7] T. Tran, R. deQueiroz, and T. Nguyen, "Linear-phase perfect reconstruction filter bank: Lattice structure, design and application in image coding," *IEEE Trans. Signal Processing*, vol. 48, pp. 133–147, Jan. 2000.
- [8] K. R. Rao and P. Yip, *Discrete Cosine Transform: Algorithms, Advantages, Applications*. San Diego, CA: Academic, 1990.
- [9] P. P. Vaidyanathan, *Multirate Systems and Filter Banks*. Englewood Cliffs, NJ: Prentice-Hall, 1993.
- [10] I. Daubechies, *Ten Lectures on Wavelets*. Philadelphia, PA: SIAM, 1992.
- [11] P. Steffen, P. N. Heller, R. A. Gopinath, and C. S. Burrus, "Theory of regular m -band wavelet bases," *IEEE Trans. Signal Processing*, vol. 41, pp. 3497–3510, Dec. 1993.
- [12] S. Oraintara, "Regular linear phase perfect reconstruction filter banks for image compression," Ph.D. dissertation, Boston Univ., Boston, MA, 2000.
- [13] S. Oraintara, T. Tran, P. Heller, and T. Nguyen, "Lattice structure for regular paraunitary linear phase filterbanks," *IEEE Trans. Signal Processing*, vol. 49, pp. 2659–2672, Nov. 2001.
- [14] P. P. Vaidyanathan and A. Kirac, "Results on optimal biorthogonal filter banks," *IEEE Trans. Circuits Syst. II*, vol. 45, pp. 932–947, Aug. 1998.
- [15] Y. Wisutmethangoon and T. Q. Nguyen, "A method for design of m th-band filters," *IEEE Trans. Signal Processing*, vol. 47, pp. 1669–1678, June 1999.
- [16] P. N. Heller and H. L. Resnikoff, "Regular m -band wavelets and applications," in *Proc. ICASSP*, vol. III, 1993, pp. III-229–III-232.
- [17] J. P. Princen and A. B. Bradley, "Analysis/synthesis filter bank design based on time domain aliasing cancellation," *IEEE Trans. Acoust., Speech, Signal Processing*, vol. ASSP-34, pp. 1153–1161, Oct. 1986.
- [18] T. D. Tran and T. Q. Nguyen, "On m -channel linear-phase FIR filter banks and application in image compression," *IEEE Trans. Signal Processing*, vol. 45, pp. 2175–2187, Sept. 1997.
- [19] X. Q. Gao, T. Q. Nguyen, and G. Strang, "The factorization of m -channel paraunitary filter banks," *IEEE Trans. Signal Processing*, submitted for publication.
- [20] E. Kreyszig, *Advanced Engineering Mathematics*, 8th ed. New York: Wiley, 1999.
- [21] H. Zou and A. H. Tewfik, "Discrete orthogonal m -band wavelet decompositions," in *Proc. ICASSP*, vol. 4, 1992, pp. IV-605–IV-608.
- [22] S. Oraintara, P. Heller, T. Tran, and T. Nguyen, "Lattice structure for regular-paraunitary linear-phase filter banks," in *Proc. 2nd Int. Workshop Transforms Filter Banks*, Brandenburg an der Havel, Germany, Mar. 1999.
- [23] W. Dai, T. Tran, S. Oraintara, and T. Nguyen, "Regular biorthogonal linear phase filter banks with rational coefficients," in *Proc. ISCAS*, Phoenix, AZ, May 2002.
- [24] M. Antonini, M. Barlaud, P. Mathieu, and I. Daubechies, "Image coding using wavelet transform," *IEEE Trans. Image Processing*, vol. 1, pp. 205–220, Apr. 1992.
- [25] T. D. Tran and T. Q. Nguyen, "A progressive transmission image coder using linear phase uniform filter banks as block transforms," *IEEE Trans. Image Processing*, vol. 48, pp. 1493–1507, Nov. 1999.
- [26] H. S. Malvar, "Fast progressive image coding without wavelets," in *Proc. Data Compression Conf.*, Snowbird, UT, Mar. 2000, pp. 243–252.



Soontorn Oraintara (S'97–M'00) received the B.E. degree (with first-class honors) from the King Monkut's Institute of Technology Ladkrabang, Bangkok, Thailand, in 1995 and the M.S. and Ph.D. degrees, both in electrical engineering, respectively, from the University of Wisconsin, Madison, in 1996 and Boston University, Boston, MA, in 2000.

He joined the Department of Electrical Engineering, University of Texas at Arlington (UTA), as Assistant Professor in July 2000. From May 1998 to April 2000, he was an intern and a consultant at the Advanced Research and Development Group, Ericsson Inc., Research Triangle Park, NC. His current research interests are in the field of digital signal processing: wavelets, filterbanks, and multirate systems and their applications in data compression, signal detection and estimation, communications, image reconstruction, and regularization and noise reduction.

Dr. Oraintara received the Technology Award from Boston University for his invention on Integer DCT (with Y. J. Chen and T. Q. Nguyen) in 1999. In 2003, he received the College of Engineering Outstanding Young Faculty Member Award from UTA. He represented Thailand in the International Mathematical Olympiad competitions and, respectively, received the Honorable Mention Award in Beijing, China, in 1989 and the bronze medal in Siguna, Sweden, in 1990.

Trac D. Tran (M'98) received the B.S. and M.S. degrees from the Massachusetts Institute of Technology, Cambridge, in 1994 and the Ph.D. degree from the University of Wisconsin, Madison, in 1998, all in electrical engineering.

He joined the Department of Electrical and Computer Engineering, The Johns Hopkins University, Baltimore, MD, in July 1998 as Assistant Professor. His current research interests are in the field of digital signal processing; particularly in multirate systems, filterbanks, wavelets, transforms, and their applications in signal representation, compression, processing, and communications.

Dr. Tran was the co-director of the 33rd Annual Conference on Information Sciences and Systems (CISS'99), Baltimore, MD, in March 1999. He received the NSF CAREER award in 2001.

Truong Q. Nguyen (SM'98) received the B.S., M.S., and Ph.D. degrees in electrical engineering from the California Institute of Technology, Pasadena, in 1985, 1986, and 1989, respectively.

He was with the Lincoln Laboratory, Massachusetts Institute of Technology (MIT), Lexington, from June 1989 to July 1994, as a member of technical staff. From 1993 to 1994, he was a visiting lecturer at MIT and an adjunct professor at Northeastern University, Boston, MA. From August 1994 to July 1998, he was with the Electrical and Computer Engineering Department, University of Wisconsin, Madison. He was with Boston University, Boston, MA, from 1996 to 2001. He is now a Full Professor at the University of California, San Diego. His research interests are in the theory of wavelets and filterbanks and applications in image and video compression, telecommunications, bioinformatics, medical imaging and enhancement, and analog/digital conversion. He is the coauthor (with Prof. G. Strang) of a popular textbook entitled *Wavelets and Filter Banks* (Wellesley, MA: Wellesley-Cambridge 1997), and the author of several matlab-based toolboxes on image compression, electrocardiogram compression, and filterbank design. He also holds a patent on an efficient design method for wavelets and filterbanks and several patents on wavelet applications, including compression and signal analysis.

Prof. Nguyen received the IEEE TRANSACTIONS ON SIGNAL PROCESSING Paper Award (in the Image and Multidimensional Processing area) for the paper he co-wrote with Prof. P. P. Vaidyanathan on linear-phase perfect-reconstruction filterbanks in 1992. He received the NSF Career Award in 1995 and is currently the Series Editor (Digital Signal Processing) for Academic Press. He served as Associate Editor for the IEEE TRANSACTIONS ON SIGNAL PROCESSING from 1994 to 1996 and for the IEEE TRANSACTIONS ON CIRCUITS AND SYSTEMS from 1996 to 1997. He received the Technology Award from Boston University for his invention on Integer DCT (with Y. J. Chen and S. Oraintara). He co-organizes (with Prof. G. Strang at MIT) several workshops on wavelets and has also served on the DSP Technical Committee for the IEEE Circuits and Systems Society.